Received: 8 October 2022 | Accepted: 25 January 2023

DOI: 10.1002/pamm.202200282

Computational model for the semi-analytical assessment of the free-edge effect in composite laminated shells

Andreas Kappel[1,*] and **Christian Mittelstedt**[1]

[1] Technische Universität Darmstadt, Department for Mechanical Engineering, Institute for Lightweight Construction and Design, Otto-Berndt-Str. 2, 64287 Darmstadt, Germany

The development of efficient computational models for the accurate prediction of the state variables in general composite laminated shells undergoing uniform edge loadings is a major challenge, especially when stress concentration phenomena such as the free-edge effect have to be considered. This paper addresses this issue by introducing a higher-order semi-analytical approach for the assessment of the three-dimensional stress field in circular cylindrical composite shells with arbitrary layups subjected to a uniform bending moment. The presented semi-analytical approach combines a closed-form analytical plane-strain solution with a higher-order layerwise approach, and the governing equations are derived by virtue of the principle of minimum elastic potential. The resulting system of coupled ordinary differential equations is then solved by means of the state-space approach and the free constants are determined by evaluating the boundary conditions at the traction-free edges. A comparison of the numerical results of the presented semi-analytical method with finite element simulations for various composite laminates indicates that the developed method works with high accuracy, although being extremely efficient in terms of computational resources.

1 Introduction

Besides the increasingly regulated environmental demands, primary lightweight engineering components especially have to fulfill sophisticated technical and economical requirements. It is for this reason that in the last decades, fiber-reinforced plastics have attracted more and more attention due to their favourable specific material properties and their ability to arbitrarily tailor the stacking sequence of composite laminates in order to meet given design aims. Several experimental investigations of composite laminated shells undergoing different loading conditions revealed [1], however, that those safety-critical structures exhibit complex failure modes with an interaction of matrix cracking and delamination mainly called forth due to three-dimensional stress concentrations at the traction-free edges between adjacent unidirectional reinforced laminate layers. This phenomenon, commonly referred to as the free-edge effect, is omnipresent since it is a consequence of the varying deformation properties of composite structures and thus, has to be taken into consideration throughout the whole development process.
In order to increase the efficiency of the design process of curved composite laminated shells undergoing different mechanical loadings, corresponding two-dimensional closed-form analytical solutions can be utilized [2, 3]. Although those methods enable a cost-effective determination of the state variables, they are not capable of depicting the stress field in the boundary-layer region of these components. For this reason, the assessment of the free-edge effect is usually carried out by means of full-scale three-dimensional finite element computations which, however, are most often unfavourable in terms of the required computational resources. Higher-order displacement-based layerwise approaches, on the other hand, represent a genuine alternative to getting an insight into the free-edge effect since they deliver results of similar quality needing only a fraction of the required computational resources of the numerical simulations [4, 5].
This contribution presents a semi-analytical model that is an extension of the method introduced by Kappel and Mittelstedt [4] and an updated version of the model discussed in [6]. The stress field of the considered composite laminated shells undergoing four-point bending loading conditions is computed by taking the generalized displacement field of a cylindrical body and modifying it by superimposing a priori unknown displacement functions which are combined with Lagrangian interpolation functions. By virtue of the minimum total potential energy principle, the governing equations as well as the admissible boundary conditions at the traction-free edges can be derived in a closed-form manner, leading to a quadratic eigenvalue problem that has to be solved numerically. The stress field of the composite laminated shell computed by the semi-analytical method is verified by comparison with three-dimensional finite element simulations carried out using the commercial tool Abaqus.

2 Structural situation

In this contribution, circular cylindrical composite laminated shells of finite length with N perfectly bonded, homogeneous laminate layers reinforced by unidirectional fibers are considered (see Fig. 1). The radius of the mid-plane and the total thickness are specified by means of R and h, while $2\theta_0$ defines the opening angle and $2z_0$ refers to the length of the analysed

* Corresponding author: e-mail andreas.kappel@klub.tu-darmstadt.de, phone +49 6151 16 220 20, fax +49 6151 16 219 80

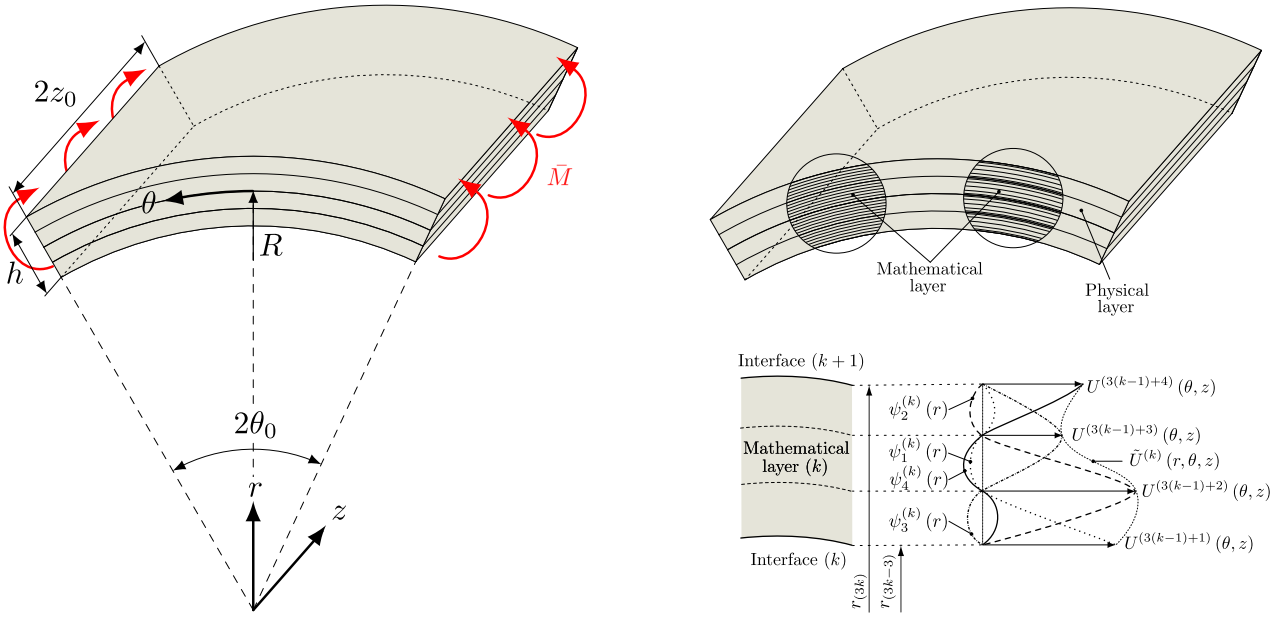

Fig. 1: Structural situation (left) and discretization of the considered composite laminated shell with an exemplary representation of the radial displacement function $U(r,z)$ (right) [5, 6]

composite shells. All laminate layers are expected to have the same ply thickness $d_L = 0.25\,\text{mm}$. The unidirectional fibers of a $0°$-ply run along the circumferential direction θ. The considered composite laminated shells will have traction-free edges at the axial positions $z = 0,\ 2z_0$ and are subjected to a uniform bending moment flux $\bar{M}$ at its circumferential ends $\theta = \pm\theta_0$. Consequently, the stress, as well as strain field, is expected to show a rotational symmetry along the circumferential direction θ. All computations are carried out within the framework of geometric as well as physical linearity.

3 Semi-analytical model

In the upcoming derivation, we consider the three-dimensional theory of linear elasticity wherein the bending moment flux $\bar{M}$ is constant along the axial direction z. Consequently, a generalized plane state of strain at a sufficient distance from the traction-free edge is obtained and we can make use of the following modified displacement field for the k^{th} mathematical layer (see Fig. 1) [5]:

$$u^{(k)}(r,\theta,z) = U_\infty^{(l(k))}(r) + \sum_j U^{(j)}(\theta,z)\,\Phi^{(j)}(r) + u_0\cos(\theta) + v_0\sin(\theta) \tag{1}$$

$$v^{(k)}(r,\theta,z) = V_\infty^{(l(k))}(r,\theta) + \sum_j \left(V^{(j)}(\theta,z) - U^{(j)}(\theta,z)\right)\Phi^{(j)}(r) - u_0\sin(\theta) + v_0\cos(\theta) + \omega_3 r \tag{2}$$

$$w^{(k)}(r,\theta,z) = W_\infty^{(l(k))}(r,\theta) + \sum_j W^{(j)}(\theta,z)\,\Phi^{(j)}(r) + w_0, \tag{3}$$

with $j \in \{I(k)+1, ..., I(k)+\Psi+1\}$. Herein, Ψ defines the order of the global Lagrangian interpolation vector $\Phi^{(j)}(r)$ which is comprised of all local shape functions $\psi^{(k)}$ utilized in the course of the semi-analytical computation and $I(k) = \psi^{(k)}(k-1)$ describes the last grid point of the $(k-1)^{th}$ mathematical layer (see Fig. 1) [4, 5].
The displacement components $u^{(k)}(r,\theta,z)$, $v^{(k)}(r,\theta,z)$ and $w^{(k)}(r,\theta,z)$ refer to the radial, circumferential and axial displacements of a material point located at (r,θ,z) in the k^{th} mathematical layer of the composite laminated shell. The rigid-body translations u_0, v_0 and w_0 in all three dimensions and the rigid-body rotation ω_3 about the z-axis are specified by the underlying displacement boundary conditions. Further on, the displacement functions $U_\infty^{(l(k))}(r)$, $V_\infty^{(l(k))}(r,\theta)$ and $W_\infty^{(l(k))}(r,\theta)$ characterize the local displacements of an individual laminate ply $l(k)$ in the corresponding k^{th} mathematical layer. They are derived in a closed-form manner by utilizing the following stress functions $F^{(l(k))}$ and $\Psi^{(l(k))}$ [5, 6]:

$$F^{(l(k))}(r) = C_1^{(l(k))} r^2 + C_2^{(l(k))} r + C_3^{(l(k))} r^{1+\lambda^{(l(k))}} + C_4^{(l(k))} r^{1-\lambda^{(l(k))}} \tag{4}$$

$$\Psi^{(l(k))}(r) = 2C_1^{(l(k))}\eta_1^{(l(k))} r + C_2^{(l(k))}\eta_2^{(l(k))}\ln(r) + C_3^{(l(k))}\eta_\lambda^{(l(k))} r^{\lambda^{(l(k))}} + C_4^{(l(k))}\eta_{-\lambda}^{(l(k))} r^{-\lambda^{(l(k))}}, \tag{5}$$

wherein the material parameters $\lambda^{(l(k))}$, $\eta_1^{(l(k))}$, $\eta_2^{(l(k))}$ and $\eta_{\pm\lambda}^{(l(k))}$

$$\lambda^{(l(k))} = \frac{\tilde{S}_{11}^{(l(k))}\tilde{S}_{44}^{(l(k))} - \tilde{S}_{14}^{(l(k))}\tilde{S}_{14}^{(l(k))}}{\tilde{S}_{22}^{(l(k))}\tilde{S}_{44}^{(l(k))} - \tilde{S}_{24}^{(l(k))}\tilde{S}_{24}^{(l(k))}}, \tag{6}$$

$$\eta_1^{(l(k))} = \frac{\tilde{S}_{14}^{(l(k))} + \tilde{S}_{24}^{(l(k))}}{\tilde{S}_{44}^{(l(k))}}, \quad \eta_2^{(l(k))} = \frac{\tilde{S}_{11}^{(l(k))} + \tilde{S}_{24}^{(l(k))}}{\tilde{S}_{14}^{(l(k))}}, \quad \eta_{\pm\lambda}^{(l(k))} = \pm\frac{\tilde{S}_{14}^{(l(k))} \pm \tilde{S}_{24}^{(l(k))}\lambda^{(l(k))}}{\tilde{S}_{44}^{(l(k))}}\frac{1 \pm \lambda^{(l(k))}}{\lambda^{(l(k))}}, \tag{7}$$

are computed by means of the reduced compliance constants $\tilde{S}_{ij}^{(l(k))}$:

$$\tilde{S}_{ij}^{(l(k))} = S_{ij}^{(l(k))} - \frac{S_{i3}^{(l(k))}S_{j3}^{(l(k))}}{S_{33}^{(l(k))}} \tag{8}$$

Consequently, the stress field is obtained as follows:

$$\begin{aligned}
&\sigma_{rr,\infty}^{(l(k))}(r) = \frac{1}{r}\frac{dF^{(l(k))}}{dr}, \quad \sigma_{\theta\theta,\infty}^{(l(k))}(r) = \frac{d^2F^{(l(k))}}{dr^2}, \quad \tau_{\theta z,\infty}^{(l(k))}(r) = -\frac{d\Psi^{(l(k))}}{dr}, \\
&\sigma_{zz,\infty}^{(l(k))}(r) = -\frac{1}{S_{33}^{(l(k))}}\left(S_{13}^{(l(k))}\sigma_{rr,\infty}^{(l(k))} + S_{23}^{(l(k))}\sigma_{\theta\theta,\infty}^{(l(k))} + S_{34}^{(l(k))}\tau_{\theta z,\infty}^{(l(k))}\right)
\end{aligned} \tag{9}$$

The shear stress components $\tau_{rz,\infty}^{(l(k))}$ and $\tau_{r\theta,\infty}^{(l(k))}$ vanish due to the rotational symmetry of the underlying structural situation. Finally, through the kinematics of the circular cylindrical composite laminated shell and Hooke's generalized material law, the displacement functions $U_\infty^{(l(k))}(r)$, $V_\infty^{(l(k))}(r,\theta)$ and $W_\infty^{(l(k))}(r,\theta)$ can be specified in a closed-form manner:

$$U_\infty^{(l(k))}(r) = \int_r \left(\tilde{S}_{11}^{(l(k))}\sigma_{rr,\infty}^{(l(k))} + \tilde{S}_{12}^{(l(k))}\sigma_{\theta\theta,\infty}^{(l(k))} + \tilde{S}_{14}^{(l(k))}\tau_{\theta z,\infty}^{(l(k))}\right) dr \tag{10}$$

$$V_\infty^{(l(k))}(r,\theta) = \int_\theta \left(r\left(\tilde{S}_{12}^{(l(k))}\sigma_{rr,\infty}^{(l(k))} + \tilde{S}_{22}^{(l(k))}\sigma_{\theta\theta,\infty}^{(l(k))} + \tilde{S}_{24}^{(l(k))}\tau_{\theta z,\infty}^{(l(k))}\right) - U_\infty^{(l(k))}(r)\right) d\theta \tag{11}$$

$$W_\infty^{(l(k))}(r,\theta) = \int_\theta r\left(\tilde{S}_{14}^{(l(k))}\sigma_{rr,\infty}^{(l(k))} + \tilde{S}_{24}^{(l(k))}\sigma_{\theta\theta,\infty}^{(l(k))} + \tilde{S}_{44}^{(l(k))}\tau_{\theta z,\infty}^{(l(k))}\right) d\theta \tag{12}$$

By utilizing the admissible boundary and continuity conditions, the $4N$ constants can be determined [6].
The displacement functions $\tilde{U}^{(j)}(r,\theta,z)$, $\tilde{V}^{(j)}(r,\theta,z)$ and $\tilde{W}^{(j)}(r,\theta,z)$, on the other hand, are specified through a separation approach wherein the local shape functions $\psi^{(k)}(r)$ are multiplied with the corresponding two-dimensional displacement functions $U^{(j)}(\theta,z)$, $V^{(j)}(\theta,z)$ and $W^{(j)}(\theta,z)$.
Making use of the underlying kinematics

$$\begin{aligned}
&\varepsilon_{rr}^{(k)} = \frac{\partial u^{(k)}}{\partial r}, \quad \varepsilon_{\theta\theta}^{(k)} = \frac{1}{r}\left(\frac{\partial v^{(k)}}{\partial\theta} + u^{(k)}\right), \quad \varepsilon_{zz}^{(k)} = \frac{\partial w^{(k)}}{\partial z}, \\
&\gamma_{\theta z}^{(k)} = \frac{\partial v^{(k)}}{\partial z} + \frac{1}{r}\frac{\partial w^{(k)}}{\partial\theta}, \quad \gamma_{rz}^{(k)} = \frac{\partial w^{(k)}}{\partial r} + \frac{\partial u^{(k)}}{\partial z}, \quad \gamma_{r\theta}^{(k)} = \frac{1}{r}\left(\frac{\partial u^{(k)}}{\partial\theta} - v^{(k)}\right) + \frac{\partial v^{(k)}}{\partial r}
\end{aligned} \tag{13}$$

and Hooke's generalized law for each mathematical layer (k)

$$\begin{pmatrix} \varepsilon_{rr}^{(k)} \\ \varepsilon_{\theta\theta}^{(k)} \\ \varepsilon_{zz}^{(k)} \\ \gamma_{\theta z}^{(k)} \\ \gamma_{rz}^{(k)} \\ \gamma_{r\theta}^{(k)} \end{pmatrix} = \begin{bmatrix} S_{11}^{(k)} & S_{12}^{(k)} & S_{13}^{(k)} & S_{14}^{(k)} & 0 & 0 \\ S_{12}^{(k)} & S_{22}^{(k)} & S_{23}^{(k)} & S_{24}^{(k)} & 0 & 0 \\ S_{13}^{(k)} & S_{23}^{(k)} & S_{33}^{(k)} & S_{34}^{(k)} & 0 & 0 \\ S_{14}^{(k)} & S_{24}^{(k)} & S_{34}^{(k)} & S_{44}^{(k)} & 0 & 0 \\ 0 & 0 & 0 & 0 & S_{55}^{(k)} & S_{56}^{(k)} \\ 0 & 0 & 0 & 0 & S_{56}^{(k)} & S_{66}^{(k)} \end{bmatrix} \begin{pmatrix} \sigma_{rr}^{(k)} \\ \sigma_{\theta\theta}^{(k)} \\ \sigma_{zz}^{(k)} \\ \tau_{\theta z}^{(k)} \\ \tau_{rz}^{(k)} \\ \tau_{r\theta}^{(k)} \end{pmatrix}, \tag{14}$$

these unknown displacement functions can be determined by virtue of the minimum total potential energy principle [4]:

$$\begin{aligned}
\delta\Pi =& \delta\Pi_i + \delta\Pi_e \\
=& \frac{1}{2}\sum_k \int_0^{2z_0}\int_{-\theta_0}^{\theta_0}\int_{r_{(k-1)}}^{r_{(k)}} \delta\underline{\varepsilon}^{(k)^T}\underline{\sigma}^{(k)} r\, dr\, d\theta\, dz - \frac{1}{2}\sum_k \int_0^{2z_0}\int_{r_{(k-1)}}^{r_{(k)}} \bar{M}\delta\left(\frac{\partial v^{(k)}}{\partial r}\right) dr\, dz = 0
\end{aligned} \tag{15}$$

Employing the Euler-Lagrange equations yields the following equilibrium equations for each grid point (i) of the cylindrical composite laminated shell:

$$\begin{aligned}\delta U^{(i)}:\ \sum_j \Bigg(& -A_{55}^{ij\,(k)}\frac{d^2U^{(j)}}{dz^2} + \Big(-\bar{A}_{14}^{ji\,(k)} + \bar{A}_{56}^{ij\,(k)} - B_{24}^{ij\,(k)} - B_{56}^{ij\,(k)}\Big)\frac{dU^{(j)}}{dz} + \Big(\bar{A}_{14}^{ji\,(k)} - \bar{A}_{56}^{ij\,(k)} + \\ & B_{24}^{ij\,(k)} + B_{56}^{ij\,(k)}\Big)\frac{dV^{(j)}}{dz} + \Big(\bar{A}_{13}^{ji\,(k)} - \bar{A}_{55}^{ij\,(k)} + B_{23}^{ij\,(k)}\Big)\frac{dW^{(j)}}{dz} + \Big(\tilde{A}_{11}^{ij\,(k)} + \bar{B}_{12}^{ij\,(k)} + \\ & \bar{B}_{12}^{ji\,(k)} + D_{22}^{ij\,(k)}\Big)U^{(j)} = -M_{r,\infty}^{(i)} - N_{\theta,\infty}^{(i)}\end{aligned} \tag{16}$$

$$\begin{aligned}\delta V^{(i)}:\ \sum_j \Bigg(& A_{44}^{ij\,(k)}\frac{d^2U^{(j)}}{dz^2} - A_{44}^{ij\,(k)}\frac{d^2V^{(j)}}{dz^2} - A_{34}^{ij\,(k)}\frac{d^2W^{(j)}}{dz^2} + \Big(-\bar{A}_{14}^{ij\,(k)} + \bar{A}_{56}^{ji\,(k)} - B_{24}^{ij\,(k)} - \\ & B_{56}^{ij\,(k)}\Big)\frac{dU^{(j)}}{dz} + \Big(-\tilde{A}_{66}^{ij\,(k)} + \bar{B}_{66}^{ij\,(k)} + \bar{B}_{66}^{ji\,(k)} - D_{66}^{ij\,(k)}\Big)U^{(j)} + \Big(\tilde{A}_{66}^{ij\,(k)} - \bar{B}_{66}^{ij\,(k)} - \\ & \bar{B}_{66}^{ji\,(k)} + D_{66}^{ij\,(k)}\Big)V^{(j)} + \Big(\tilde{A}_{56}^{ij\,(k)} - \bar{B}_{56}^{ij\,(k)}\Big)W^{(j)}\Bigg) = -\bar{M}^{(i)}\end{aligned} \tag{17}$$

$$\begin{aligned}\delta W^{(i)}:\ \sum_j \Bigg(& A_{34}^{ij\,(k)}\frac{d^2U^{(j)}}{dz^2} - A_{34}^{ij\,(k)}\frac{d^2V^{(j)}}{dz^2} - A_{33}^{ij\,(k)}\frac{d^2W^{(j)}}{dz^2} + \Big(\bar{A}_{55}^{ji\,(k)} - \bar{A}_{13}^{ij\,(k)} - B_{23}^{ij\,(k)}\Big)\frac{dU^{(j)}}{dz} + \\ & \Big(-\tilde{A}_{56}^{ij\,(k)} + \bar{B}_{56}^{ji\,(k)}\Big)U^{(j)} + \Big(\tilde{A}_{56}^{ij\,(k)} - \bar{B}_{56}^{ji\,(k)}\Big)V^{(j)} + \tilde{A}_{55}^{ij\,(k)}W^{(j)}\Bigg) = 0\end{aligned} \tag{18}$$

with $j \in \{I\,(k)+1, ..., I\,(k)+\Psi+1\}$. The abbreviations can be found in appendix A.
Equations (16) - (18) characterize a system of coupled ordinary differential equations that can be solved numerically by making use of the state-space approach [4, 5].
For the boundary conditions at the traction-free edges, on the other hand, the following formulations are obtained:

$$\delta U^{(i)}:\ \sum_j \left(a_{55}^{ij\,(k)}\frac{dU^{(j)}}{dz} + \left(\bar{a}_{56}^{ij\,(k)} - b_{56}^{ij\,(k)}\right)\left(V^{(j)} - U^{(j)}\right) + \bar{a}_{55}^{ij\,(k)}W^{(j)}\right)\Bigg|_{z=0}^{z=2z_0} = 0 \tag{19}$$

$$\delta V^{(i)}:\ \sum_j \left(a_{44}^{ij\,(k)}\left(\frac{dV^{(j)}}{dz} - \frac{dU^{(j)}}{dz}\right) + a_{34}^{ij\,(k)}\frac{dW^{(j)}}{dz} + \left(\bar{a}_{14}^{ij\,(k)} + b_{24}^{ij\,(k)}\right)U^{(j)}\right)\Bigg|_{z=0}^{z=2z_0} = -R_{\theta z,\infty}^{(i)} \tag{20}$$

$$\delta W^{(i)}:\ \sum_j \left(a_{34}^{ij\,(k)}\left(\frac{dV^{(j)}}{dz} - \frac{dU^{(j)}}{dz}\right) + a_{33}^{ij\,(k)}\frac{dW^{(j)}}{dz} + \left(\bar{a}_{13}^{ij\,(k)} + b_{23}^{ij\,(k)}\right)U^{(j)}\right)\Bigg|_{z=0}^{z=2z_0} = -M_{z,\infty}^{(i)} \tag{21}$$

with $j \in \{I\,(k)+1, ..., I\,(k)+\Psi+1\}$. This concludes the derivation of the semi-analytical approach.

4 Verification of accuracy

The following section provides an insight into the accuracy of the presented semi-analytical method by studying the stress field for an unbalanced and unsymmetric $[0°/45°/30°/90°]$ composite laminated shell and by comparing the numerical results to highly detailed finite element analyses. For this, the following material properties

$$E_1 = 143\,\text{GPa},\ E_2 = E_3 = 9.1\,\text{GPa},\ G_{23} = 4.82\,\text{GPa},\ G_{12} = G_{13} = 4.9\,\text{GPa},\ \nu_{12} = \nu_{13} = \nu_{23} = 0.3$$

as well as non-dimensional quanities have been considered [5]:

$$\bar{\sigma}_{ii} = \frac{2z_0h}{\bar{M}}\sigma_{ii}, \quad \bar{\tau}_{ij} = \frac{2z_0h}{\bar{M}}\tau_{ij}, \quad \bar{r} = \frac{r-R}{h}, \quad \bar{z} = \frac{z-z_0}{2z_0}$$

with $(i, j = r, \theta, z)$. Fig. 2 depicts the stress field of the considered composite laminated shell at a sufficient distance from the boundary-layer region while Fig. 3 and Fig. 4 provide an insight into the decaying behavior of the inter- and intralaminar stress gradients from one traction-free edge at $\bar{z} = -0.5$ to $\bar{z} = 0.5$. Besides some negligible deviations due to the assumptions made in the course of the derivation, it can be concluded that even for unbalanced and unsymmetric composite laminated shells, the semi-analytical model delivers reliable results for all stress components when compared to full-scale finite element computations.

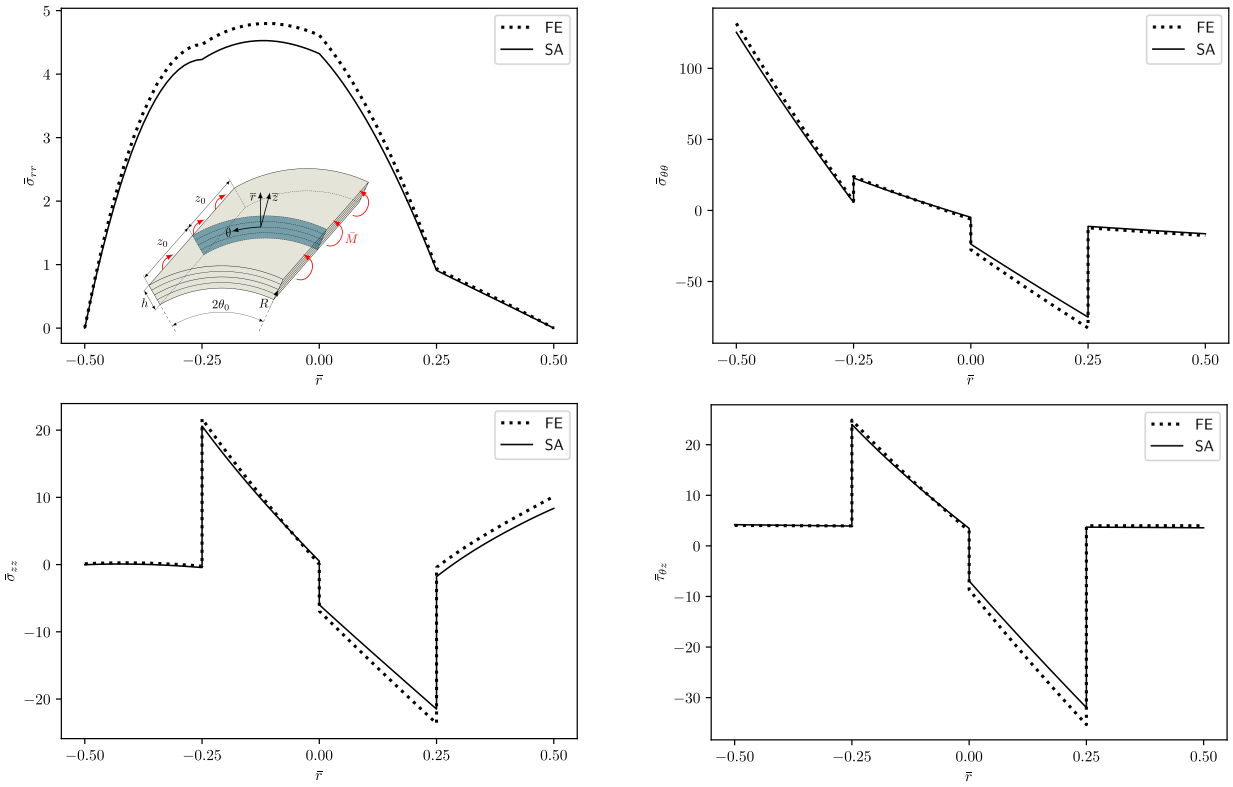

Fig. 2: Non-dimensional stress components $\bar{\sigma}_{rr}$, $\bar{\sigma}_{\theta\theta}$, $\bar{\sigma}_{zz}$ and $\bar{\tau}_{\theta z}$ evaluated at $(\theta, \bar{z}) = (0, 0)$ for the unsymmetric and unbalanced $[0°/45°/30°/90°]$ composite laminate $(R/h = 4, 2z_0/h = 4, 2\theta_0 = \pi/2)$ subjected to a uniform bending moment flux $\bar{M} = 10N$

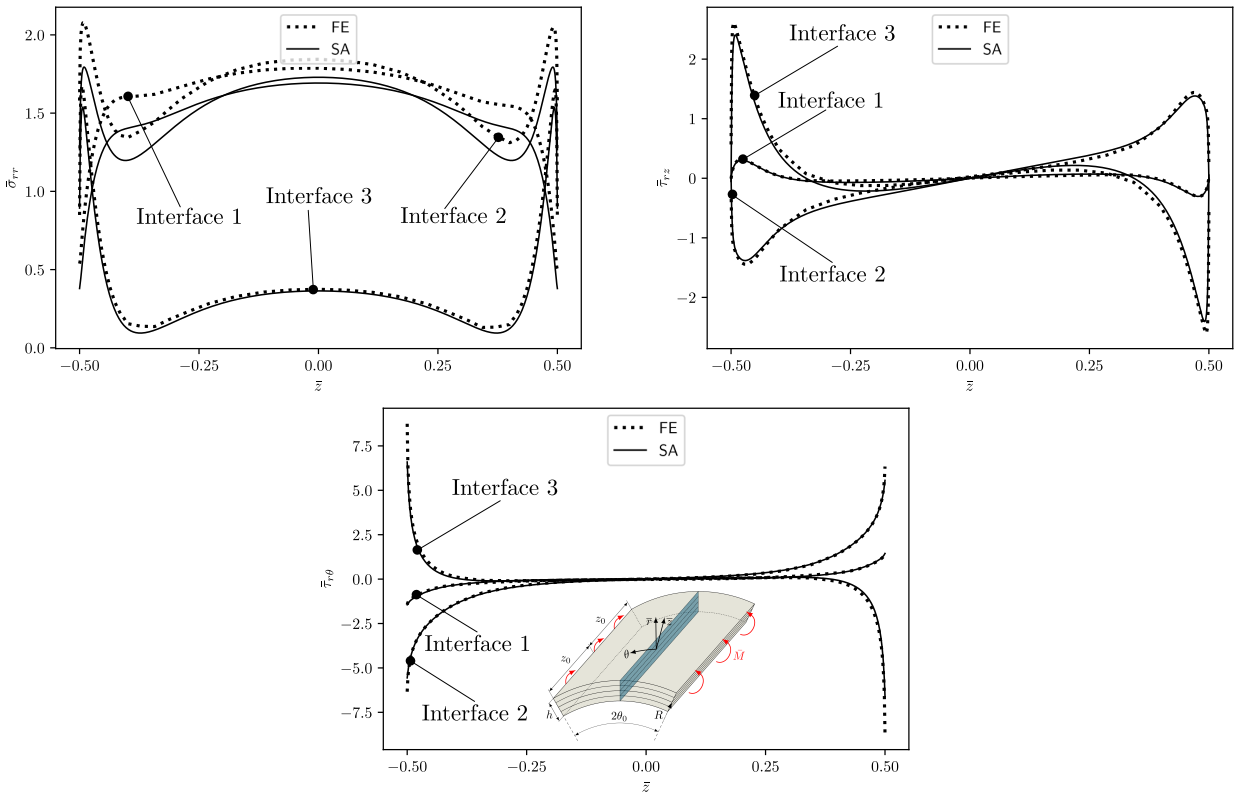

Fig. 3: Non-dimensional stress components $\bar{\sigma}_{rr}$, $\bar{\tau}_{rz}$ and $\bar{\tau}_{r\theta}$ evaluated in interface 1 at $(\bar{r} = -0.25, \theta = 0)$, in interface 2 at $(\bar{r} = 0, \theta = 0)$ and in interface 3 at $(\bar{r} = 0.25, \theta = 0)$ for the $[0°/45°/30°/90°]$ composite laminate $(R/h = 4, 2z_0/h = 4, 2\theta_0 = \pi/2)$ subjected to a uniform bending moment flux $\bar{M} = 10N$

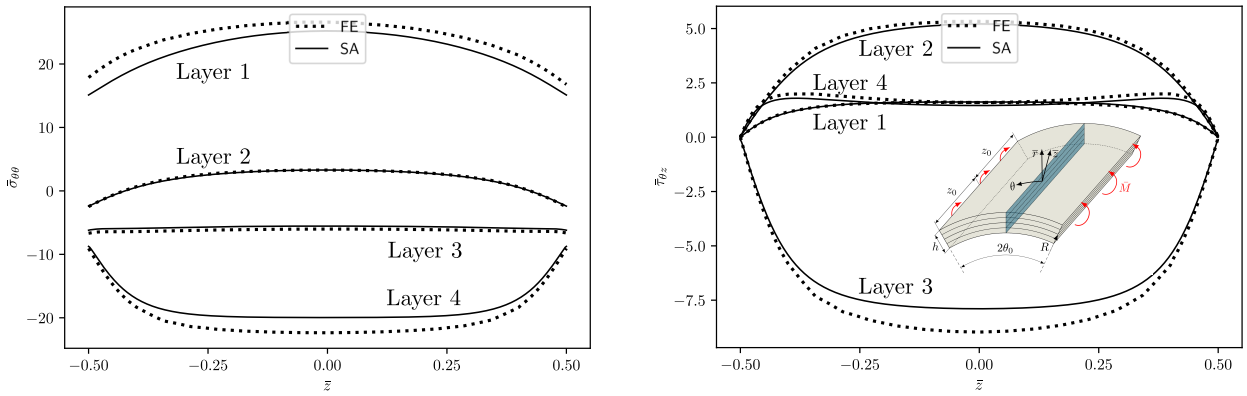

Fig. 4: Non-dimensional stress components $\bar{\sigma}_{\theta\theta}$ and $\bar{\tau}_{\theta z}$ evaluated in layer 1 at $(\bar{r} = -0.375, \theta = 0)$, in layer 2 at $(\bar{r} = -0.125, \theta = 0)$, in layer 3 at $(\bar{r} = 0.125, \theta = 0)$ and in layer 4 at $(\bar{r} = 0.375, \theta = 0)$ for the $[0°/45°/30°/90°]$ composite laminate $(R/h = 4, 2z_0/h = 4, 2\theta_0 = \pi/2)$ subjected to a uniform bending moment flux $\bar{M} = 10N$

5 Concluding remarks

In this contribution, a semi-analytical approach for the assessment of the free-edge stress fields in thick, finite length, circular cylindrical composite laminated shells subjected to a uniform bending moment has been introduced. The presented numerical results for an unbalanced and unsymmetric composite laminated shell indicated an excellent agreement when compared with highly detailed, three-dimensional finite element computations.
Further research concerning the extension of the current semi-analytical method should be conducted to assess the prediction of the free-edge stress field in general composite laminated shells undergoing arbitrary mechanical and thermal loadings.

A Abbreviations

$$\left\{A_{op}^{mn\ (k)}, \bar{A}_{op}^{mn\ (k)}, \tilde{A}_{op}^{mn\ (k)}\right\} = \int_{r_{(k-1)}}^{r_{(k)}} C_{op}^{(k)} \left\{\Phi^{(m)}\Phi^{(n)}, \Phi^{(m)}\Phi_{,r}^{(n)}, \Phi_{,r}^{(m)}\Phi_{,r}^{(n)}\right\} dr \tag{22}$$

$$\left\{B_{op}^{mn\ (k)}, \bar{B}_{op}^{mn\ (k)}, D_{op}^{mn\ (k)}\right\} = \int_{r_{(k-1)}}^{r_{(k)}} C_{op}^{(k)} \left\{\Phi^{(m)}\Phi^{(n)}, \Phi^{(m)}\Phi_{,r}^{(n)}, \Phi^{(m)}\Phi^{(n)}\frac{1}{r}\right\} \frac{1}{r}\, dr \tag{23}$$

$$\left\{a_{op}^{mn\ (k)}, \bar{a}_{op}^{mn\ (k)}, b_{op}^{mn\ (k)}\right\} = \int_{r_{(k-1)}}^{r_{(k)}} C_{op}^{(k)} \left\{\Phi^{(m)}\Phi^{(n)}, \Phi^{(m)}\Phi_{,r}^{(n)}, \Phi^{(m)}\Phi^{(n)}\frac{1}{r}\right\} r\, dr \tag{24}$$

$$\{N_{\theta,\infty}^{(i)}, M_{z,\infty}^{(i)}, R_{\theta z,\infty}^{(i)}, \bar{M}^{(i)}\} = \int_{r_{(k-1)}}^{r_{(k)}} \{\sigma_{\theta\theta,\infty}^{(k)}, r\sigma_{zz,\infty}^{(k)}, r\tau_{\theta z,\infty}^{(k)}, \bar{M}\}\Phi^{(i)}\, dr \tag{25}$$

$$\{M_{r,\infty}^{(i)}\} = \int_{r_{(k-1)}}^{r_{(k)}} \{r\sigma_{rr,\infty}^{(k)}\}\Phi_{,r}^{(i)}\, dr \tag{26}$$

Acknowledgements This work was supported by the German Research Foundation DFG [PNO 427624054]. Open access funding enabled and organized by Projekt DEAL.

References

[1] C. Mittelstedt, W. Becker, A. Kappel, and N. Kharghani, Applied Mechanics Reviews **74(1)**, 010801 (2022).
[2] J. G. Ren, Composites Science and Technology, **29(3)**, 169-187, (1987).
[3] F. G. Yuan, Journal of reinforced plastics and composites, **11(4)**, 340-371, (1992).
[4] A. Kappel, and C. Mittelstedt, Composites Part B: Engineering **183**, 107693 (2020).
[5] A. Kappel, S. Dillen, and C. Mittelstedt, Mechanics of Advanced Materials and Structures, 1-18 (2021).
[6] A. Kappel, and C. Mittelstedt, Proceedings 20th European Conference on Composite Materials, Lausanne, Switzerland, in press.

